International Journal of Pharmaceutics 683 (2025) 126007

Contents lists available at ScienceDirect

International Journal of Pharmaceutics

journal homepage: www.elsevier.com/locate/ijpharm

Impact of spin-freezing parameters and excipient composition on product stability of a PEGylated peptide formulation

Zarah Schaal [a,b], Pieter-Jan Van Bockstal [a], Joris Lammens [a], Julian H. Lenger [c,1], Adrian P. Funke [d], Stefan C. Schneid [c], Thomas De Beer [a,b,*]

[a] RheaVita, Poortakkerstraat 9C, 9051 Ghent, Belgium
[b] Laboratory of Pharmaceutical Process Analytical Technology, Department of Pharmaceutical Analysis, Faculty of Pharmaceutical Sciences, Ghent University, 9000 Ghent, Belgium
[c] Bayer AG, Pharmaceuticals, CMC Drug Product, Friedrich-Ebert-Str. 475, 42117 Wuppertal, Germany
[d] Bayer AG, Pharmaceuticals, CMC Process Engineering & Technologies, Müllerstr. 178, 13353 Berlin, Germany

ARTICLE INFO

Keywords:
Continuous freeze-drying
Biopharmaceuticals
Peptide stability
Lyophilization
Peptide glycation
Maillard reaction

ABSTRACT

This study examines the impact of spin-freezing parameters, as applied in continuous spin-freeze-drying processes, and formulation composition on the stability of a PEGylated peptide following freeze-drying and storage. A trehalose-based reference formulation was compared with two reformulated systems in which trehalose was replaced by either mannitol or a 75:25 sucrose–mannitol blend. Samples were processed under four distinct spin-freezing conditions, varying in cooling and crystallization rates, followed by batch-drying and storage at either 2–8 °C or 50 °C for up to 13 weeks. Product quality was evaluated by assessing peptide concentration, monomer content, and cake morphology. Across all formulations and storage conditions, variations in spin-freezing parameters exhibited no consistent or statistically significant effect on peptide or monomer levels. In contrast, formulation composition emerged as the dominant stability determinant. Trehalose-based samples maintained robust stability under both refrigerated storage and stress conditions, whereas mannitol-based samples exhibited moderate degradation at elevated temperatures. The sucrose–mannitol formulation demonstrated pronounced instability at 50 °C, characterized by cake collapse, browning, and interference in peptide quantification, likely as a result of sucrose hydrolysis and the formation of aromatic degradation products. These findings highlight that, for the formulations investigated, the choice of excipient is critical for product stability and that systems susceptible to sugar degradation may require adapted analytical approaches, as well as optimized drying protocols and storage conditions.

1. Introduction

Freeze-drying is a commonly used technology to enhance the stability and shelf-life of biologics, including peptide- and protein-based therapeutics (Abla and Mehanna, 2022). By removing water through sublimation and desorption under controlled temperature and reduced pressure, the process slows down degradation pathways such as hydrolysis and aggregation (Carpenter et al., 2002). However, the freezing stage can introduce significant physical and chemical stress, especially for complex biologics. The outcome of freeze-drying therefore depends not only on the choice of excipients but also on the design of the freeze-drying process itself (Izutsu, 2018; Kasper and Friess, 2011).

Continuous spin-freeze-drying has emerged as a promising alternative to conventional batch lyophilization, offering enhanced process efficiency and precise control at the vial level (Leys et al., 2020; Sharma et al., 2021). A central feature of this technology is spin-freezing, in which liquid-filled vials are rapidly frozen under a controlled cold gas flow while spinning. This results in thin, uniform frozen layers with larger surface area, improved heat and mass transfer, and more consistent product quality (De Meyer et al., 2015; Lammens et al., 2018).

In our previous study, we systematically explored the influence of these spin-freezing parameters using a trehalose-based PEGylated peptide formulation (Schaal et al., 2025). We demonstrated that variations in cooling and crystallization rates significantly impacted critical quality

* Corresponding author at: RheaVita, Poortakkerstraat 9C, 9051 Ghent, Belgium.
E-mail address: thomas.debeer@rheavita.com (T.D. Beer).
[1] Present affiliation: AbbVie Deutschland GmbH & Co. KG, Product Development Science & Technology, Knollstr. 50, 67061 Ludwigshafen, Germany.

https://doi.org/10.1016/j.ijpharm.2025.126007
Received 4 July 2025; Received in revised form 26 July 2025; Accepted 27 July 2025
Available online 5 August 2025

attributes such as pore structure, cake morphology, and moisture content.

However, our earlier work did not extend peptide content and monomer level assessments beyond the immediate post-drying stage, leaving the long-term implications of these parameters, especially under stress conditions, unresolved. Furthermore, the interplay between formulation composition and spin-freezing conditions has not been extensively investigated.

The present study addresses these gaps by evaluating the stability of a PEGylated peptide across three formulations: a trehalose-based reference, a mannitol-based system, and a sucrose–mannitol blend. In contrast to our earlier work, we assess peptide stability over a 13-week period under both refrigerated (2–8 °C) and stress (50 °C) storage conditions. In addition, we investigate whether short-term frozen storage at −70 °C prior to drying impacts product stability compared to freshly spin-frozen samples. The aim is to determine whether spin-freezing parameters significantly influence long-term product stability, how these effects compare across formulation compositions, and whether temporary frozen storage introduces additional variability. For this purpose, we assessed peptide concentration, monomer levels, and cake morphology under various processing and storage conditions. The findings are expected to support the development of optimized formulation and process strategies for robust spin-freeze-dried biopharmaceuticals.

2. Materials and methods

2.1. Sample preparation and handling

The study was conducted using a model peptide consisting of 52 amino acids conjugated to a 40 kDa polyethylene glycol (PEG-API, Bayer AG, Wuppertal, Germany). This API was originally developed as a conventionally lyophilized drug product formulated with trehalose dihydrate as a stabilizing excipient to maintain peptide integrity during storage. The PEG-API was formulated at a concentration of 3.7 mg/mL in a citrate-based buffer at pH 4, containing 7.5 mg/mL citrate, 1.7 mg/mL sodium chloride, and trehalose as a stabilizer at a concentration of 50 mg/mL.

To investigate the impact of formulation composition on peptide recovery under different freezing conditions, the original trehalose-based formulation was used as a reference, while two alternative formulations with slightly different compositions were prepared. In these formulations, trehalose was replaced either with a 75:25 mixture of sucrose and mannitol (both from Sigma-Aldrich, Schnelldorf, Germany) or with pure mannitol (Sigma-Aldrich, Schnelldorf, Germany), maintaining a stabilizer concentration of 50 mg/mL. All excipients were of pharmaceutical grade. For clarity, the three formulations are referred to as Trehalose (Tre), Sucrose–Mannitol (Suc–Man), and Mannitol (Man) formulations throughout the manuscript.

Each formulation was filled into 6R glass vials with a standardized filling volume of 2.28 mL and subsequently stoppered. The vials were stored at −70 °C until required for experimental use. Prior to analysis, the samples were thawed under controlled conditions to minimize variability. To ensure consistency in pre-freezing conditions, all samples were spin-frozen within two hours of thawing.

2.2. Spin-freezing and batch drying

Before processing, the samples were prepared as outlined in Section 2.1. Spin-freezing was conducted using a WB6000-D overhead spinner (Wiggens, Beijing, China) equipped with a custom vial adapter for 6R and 10R vials. The vials were rotated along their longitudinal axis at 3000 rpm while exposed to a controlled cold gas flow, which was pre-cooled via a liquid nitrogen-based heat exchanger. The freezing process followed the method described by Schaal et al. (Schaal et al., 2025).

Four different cooling and crystallization conditions were applied, specifically 5 °C/min with 592 W/kg, 50 °C/min, 592 W/kg; 5 °C/min, 5921 W/kg; and 50 °C/min, 5921 W/kg. Cooling rates were precisely regulated using an in-house application, which relied on real-time, non-contact temperature monitoring via a FLIR A655sc thermal infrared camera (Thermal Focus, Ravels, Belgium). The gas flow rate was dynamically adjusted using two Bronkhorst F-202AV mass flow controllers (FlowCor, Olen, Belgium), and all process parameters, including vial and gas temperatures as well as gas flow rates, were recorded every 0.50 s.

During the liquid cooling phase, the gas flow was controlled using proportional-integral-derivative (PID) regulation to maintain the desired cooling rate until ice nucleation and subsequent crystal growth occurred. A mechanistic heat transfer model accounted for latent heat release, dynamically adjusting the gas temperature and flow rate to ensure precise heat removal. Throughout crystallization, the gas flow rate was maintained at 100 L/min to stabilize heat transfer from the vial. The rate of heat transfer, $\dot{Q}$ (W), can be expressed using a modified form of Newton's law of cooling:

$$\dot{Q} = \pi h \emptyset_{\text{vial}} h_{\text{vial}} \left(T_{v,o} - T_{\text{gas}} \right) \tag{1}$$

where h is the heat transfer coefficient, $\emptyset_{\text{vial}}$ is the vial diameter, h_{vial} is the vial height, $T_{v,o}$ is the outer vial wall temperature, and T_{gas} is the gas temperature. In this setup, the temperature of the cooling gas T_{gas} was measured using a type-K thermocouple (Labfacility, Leeds, UK) located between the vial and the gas outlet. The outer vial wall temperature $T_{v,o}$ was continuously monitored via the IR camera. Real-time adjustments to the gas flow rate and temperature ensured that the intended cooling rate was maintained under optimal heat transfer conditions. The heat transfer coefficient for the freezing setup was determined through experimental calibration, allowing precise temperature control and accurate prediction of thermal dynamics. Further details on this calibration and the spin-freezing control mechanisms have been extensively documented by Nuytten et al. (Nuytten et al., 2021).

Once crystallization was complete, cooling continued at the designated rate until the final freezing temperature was reached. Most samples were then stored at −70 °C for several days up to approximately one week prior to drying. To investigate the potential influence of frozen storage before drying, a subset of vials were spin-frozen freshly immediately before the drying run. For these freshly spin-frozen samples, only two vials per formulation were prepared under the two most extreme spin-freezing conditions, 5 °C/min, 592 W/kg, and 50 °C/min, 5921 W/kg. One vial per condition was analysed immediately after drying (t_0), and the other after 13 weeks at 50 °C to assess potential differences in stability.

All samples underwent drying in aluminum holders on pre-cooled shelves (−50 °C) inside a Martin Christ Epsilon 2-10D LSCplus freeze-dryer (Osterode, Germany). Primary drying was conducted at −30 °C, followed by secondary drying at 30 °C with a gradual temperature increase. The final temperature was then held for 8 h, targeting a low residual moisture content. Chamber pressure was maintained at 100 μbar throughout the process, controlled using a capacitance manometer, with a Pirani gauge used for additional monitoring.

Upon completion of drying, vials were stoppered under vacuum (100 μbar) and sealed with crimp caps. Dried samples were either analysed immediately (t_0) or stored under controlled conditions. t_0 samples and samples subjected to stress testing (stored at 50 °C in a temperature-controlled laboratory drying oven under uncontrolled relative humidity conditions for 6.5 and 13 weeks) were analysed in triplicate, while reference samples stored at 2–8 °C were prepared as single vials per condition to assess long-term storage stability. Because the vials remained sealed, the internal headspace moisture was determined by the residual moisture set at the end of the lyophilization cycle.

2.3. Modulated differential scanning Calorimetry (mDSC)

The glass transition temperature of the maximally freeze-concentrated solution (T_g') for each formulation was determined using a Q2000 differential scanning calorimeter (DSC; TA Instruments, New Castle, USA) operated in modulated DSC (mDSC) mode. This technique enables the separation of reversing and non-reversing thermal events, thereby offering enhanced resolution and interpretation compared to conventional DSC. For sample preparation, hermetically sealed aluminum pans (TA Instruments, New Castle, USA) were filled with approximately 20 μL of each formulation. A nitrogen purge gas flow of 50 mL/min was applied throughout the measurement. Samples were rapidly cooled to −90 °C, held isothermally for 5 min, and then heated to 0 °C at a rate of 2 °C/min. Modulation parameters included an amplitude of 0.212 °C and a period of 40 s. The T_g' was identified as the midpoint of the reversing heat flow signal, as calculated using TRIOS software version 5.1.1 (TA Instruments, New Castle, USA).

In addition to T_g' determination, the thermal characteristics of the lyophilized products were also evaluated using the same instrument and mDSC protocol. For these measurements, approximately 8–10 mg of lyophilized material was placed in Tzero aluminum pans (TA Instruments, New Castle, USA), with an empty pan serving as the reference. The samples were heated from 0 °C to 150 °C at a rate of 2 °C/min, applying the same modulation parameters (0.212 °C amplitude, 40-second period) and nitrogen purge flow of 50 mL/min. As with T_g', the glass transition temperature (T_g) was determined from the midpoint of the reversing heat flow signal using TRIOS software.

2.4. Karl Fischer

To determine the residual moisture content of the freeze-dried samples, Karl Fischer titrations were conducted using a V30 volumetric titrator (Mettler Toledo, Schwerzenbach, Switzerland) equipped with Hydranal™-Composite 5 reagent (Sigma-Aldrich, Schnelldorf, Germany). Before starting the sample measurements, the concentration of the Karl Fischer titrant and the water content of a 1:1 mixture of Hydranal™ dry methanol (Sigma-Aldrich, Schnelldorf, Germany) and formamide (Sigma-Aldrich, Schnelldorf, Germany) were determined. Each lyophilizate was then dissolved in a defined amount of the 1:1 dry methanol-formamide solution and left to equilibrate for moisture extraction. Via a syringe, a known mass of the dissolved cake was transferred from the vial into the V30 titration beaker and analysed.

2.5. UV–Vis spectroscopy

The absorbance characteristics of the samples were assessed using a Shimadzu UV-1650PC UV–Vis spectrophotometer (Shimadzu Corporation, Nakagyo-Ku, Japan). Prior to analysis, each lyophilized sample was reconstituted with 3.3 mL of Milli-Q water and then filtered through a 0.2 μm polyethersulfone (PES) syringe filter (JT Baker, Philippsburg, USA). An aliquot of the filtered solution was subsequently diluted 1:20 with Milli-Q water. Absorbance measurements were recorded using LabSolutions UV–Vis Version 1.12 (Shimadzu Corporation, Nakagyo-Ku, Japan) at wavelengths of 280 nm and 210 nm using a 1 cm path length quartz cuvette.

2.6. Reversed-phase high-performance liquid chromatography (RP-HPLC)

Quantification of the PEGylated active pharmaceutical ingredient (PEG-API) was performed using reverse-phase high-performance liquid chromatography (RP-HPLC) on a Nexera Ultra High-Performance Liquid Chromatography (UHPLC) system (Shimadzu Corporation, Nakagyo-Ku, Japan). The instrument setup comprised an LC-40D x3 binary pump, SIL-40C x3 autosampler, DGU-403/405 degasser, CTO-40C column oven, and SPD-M40 photodiode array detector. Each analytical run included a reference sample to ensure consistency and enable normalization. Prior to injection, lyophilized samples were reconstituted in 3.3 mL of Milli-Q water and passed through a 0.2 μm polyethersulfone (PES) syringe filter (JT Baker, Philippsburg, USA) to remove particulates. A 50 μL injection volume was used for all analyses. Detection was carried out at two wavelengths: 280 nm for the quantification of PEG-API, and 210 nm for monitoring potential degradation products.

Chromatographic separation was achieved on a YMC-Triart Bio C4 column (YMC, Kyoto, Japan), maintained at 60 °C. The mobile phase consisted of 0.1 % (v/v) trifluoroacetic acid (TFA, Sigma-Aldrich, St. Louis, USA) in water (aqueous phase) and 0.1 % (v/v) TFA in acetonitrile (organic phase, Fisher Scientific, Fairlawn, NJ). A linear gradient was applied, decreasing the aqueous phase from 87 % to 40 % over 30 min, followed by a 5-minute re-equilibration step returning to 87 % aqueous phase. The flow rate was set at 0.6 mL/min. Chromatographic data were processed and analysed using LabSolutions software version 5.106 (Shimadzu Corporation, Nakagyo-Ku, Japan).

2.7. Size exclusion chromatography (SEC)

Peptide monomer levels were assessed by size exclusion chromatography (SEC) with UV detection at 280 nm. Prior to analysis, all samples, including reference controls, were reconstituted and filtered as described in Section 2.6 to ensure consistency in sample preparation. Chromatographic analysis was conducted using a Dionex Summit HPLC system (Dionex Corporation, Sunnyvale, CA, USA), equipped with a P680A pump, ASI-100 T autosampler, TCC-100 column compartment, and UVD170 UV/Vis detector. Separation was performed on a WTC-030S5 analytical column (Wyatt Technology Corporation, Santa Barbara, USA), preceded by a WTC-030S5G guard column of matching chemistry to protect against particulate or contaminant buildup.

The mobile phase consisted of 10 % (v/v) 96 % absolute ethanol (VWR, Radnor, USA) and 90 % aqueous buffer containing 50 mM sodium dihydrogen phosphate and 150 mM sodium chloride (Sigma-Aldrich, St. Louis, USA). The system was operated at a flow rate of 0.7 mL/min, with an injection volume of 30 μL per sample. The total runtime for each analysis was 30 min. Chromatographic data acquisition and evaluation were performed using Chromeleon software, version 6.8 (Dionex Corporation, Sunnyvale, USA).

3. Results and discussions

3.1. Cake appearance

The visual appearance of the freeze-dried cakes was first assessed directly after lyophilization (t_0) to evaluate the influence of formulation composition and spin-freezing conditions on cake morphology. As shown in Fig. 1, the trehalose-based reference formulation consistently yielded elegant cakes under all tested spin-freezing conditions. When processed with a low crystallization rate, surface cracking was observed. In particular, both the 5 °C/min and 50 °C/min conditions at 592 W/kg led to visible cracks, while cakes processed at a high crystallization rate (5921 W/kg) exhibited little to no cracking but showed slight shrinkage, in line with previous observations described in Schaal et al. (Schaal et al., 2025).

The mannitol formulation produced uniformly flawless cakes across all spin-freezing conditions, with no visible cracks, shrinkage, or collapse. This consistently robust appearance is attributed to the crystalline nature of mannitol, which provides strong structural support during freeze-drying. Upon freezing, mannitol typically readily crystallizes, forming a stable matrix that retains its shape throughout the drying process (Thakral et al., 2023). This reduces the risk of collapse and contributes to excellent cake morphology regardless of cooling or crystallization rate. However, mannitol typically crystallizes in a separate phase from the API and therefore does not contribute to molecular stabilization of the peptide.

Fig. 1. Cake appearance directly after lyophilization. From left to right: Trehalose, Mannitol, and Sucrose–Mannitol formulations. Each set of four vials represents one formulation processed under different spin-freezing conditions: 5 °C/min, 592 W/kg; 50 °C/min, 592 W/kg; 5 °C/min, 5921 W/kg; 50 °C/min, 5921 W/kg.

In contrast, the sucrose–mannitol formulation displayed severe cake defects across all tested conditions, with all samples exhibiting varying degrees of collapse or structural breakdown. This behavior is likely related to the physical state of mannitol in the mixture. At the 75:25 w/w sucrose–mannitol ratio used in this study, mannitol is known to remain largely amorphous when co-formulated with sucrose. Previous studies have shown that blends up to ~30 % w/w mannitol remain fully amorphous, with crystallinity first detected at ~40 % w/w and above (Al-Hussein and Gieseler, 2012; Kim et al., 1998; Thakral et al., 2023). In such cases, sucrose interferes with mannitol crystallization during freezing, resulting in a predominantly amorphous matrix that lacks the structural integrity provided by crystalline mannitol in single-component systems. Since amorphous systems generally exhibit lower collapse temperatures than their crystalline counterparts, the sucrose–mannitol formulation was likely more prone to structural collapse during drying (Meyer et al., 2009).

This interpretation aligns with Karl Fischer titration results, which revealed significantly higher residual moisture content in the sucrose–mannitol samples (~3.1 %) compared to trehalose (~0.6 %) and mannitol (~0.9 %). This elevated moisture content likely resulted from reduced surface area following partial collapse, which may have limited water removal efficiency during secondary drying. Modulated DSC analysis further indicated a relatively low T_g of ~31 °C for the sucrose–mannitol formulation, while the purely mannitol-based formulation showed distinct melting peaks at ~123 °C and ~142 °C, confirming its crystalline nature. An XRD analysis (data not shown) confirmed the presence of both the metastable δ and the stable β polymorphs, corresponding to the lower- and higher-temperature melting events, respectively. In contrast, the trehalose-based formulation displayed a T_g of ~80 °C. Although the frozen-state T_g' values were comparable across formulations (−40.6 °C for trehalose, −41.1 °C for sucrose–mannitol, and −42.6 °C for mannitol), the amorphous nature of the sucrose–mannitol matrix likely increased molecular mobility and reduced resistance to energy input. As secondary drying was conducted at 30 °C, close to the measured T_g of the sucrose-mannitol formulation, collapse may have occurred during the ramp-up phase, when residual moisture content was still elevated and the effective glass transition temperature was likely lower than the measured value. These findings suggest that the collapse was primarily driven by the formulation's predominantly amorphous nature and low T_g, in combination with the process conditions. Slightly lower secondary drying temperatures might have mitigated the risk of collapse, highlighting the combined impact of formulation properties and drying parameters.

After 13 weeks of storage at 2–8 °C, all three formulations retained their original post-drying appearance, with no visible changes in cake structure irrespective of spin-freezing parameters (Fig. 2) This confirms that refrigerated storage effectively preserved the physical integrity of the lyophilizates across all conditions.

Following storage at 50 °C for 13 weeks, the trehalose and mannitol cakes remained visually unchanged compared to their appearance directly after drying, further confirming their morphological stability (Fig. 3A+B). However, the sucrose–mannitol formulation showed additional degradation beyond the collapse already present at t_0. Notably, in Fig. 3C, the intensity of brown discoloration and the extent of structural breakdown varied with spin–freezing parameters. Samples processed at high cooling and crystallization rates exhibited the most pronounced cake collapse and darkest browning in the sucrose–mannitol formulation, suggesting that these spin–freezing settings may promote physical instability. Since the glass transition temperature of this formulation was around 31 °C, storing it at 50 °C likely caused high molecular mobility, promoting sucrose hydrolysis and subsequent degradation reactions further detailed in Section 3.2.

Interestingly, no clear differences in cake appearance were observed between formulation samples that were freshly spin-frozen and dried (Fig. 4A) versus those stored at −70 °C for one week to a few days prior to drying (Fig. 4B) irrespective of the formulation, indicating that short-term frozen storage before drying did not significantly impact cake morphology under the conditions tested.

3.2. Peptide assay

The overall peptide content was assessed using RP-HPLC, with quantification based on UV absorbance at 210 nm and 280 nm. At the initial timepoint (t_0), all three formulations showed peptide concentrations close to 100 %, confirming that the lyophilization process preserved the integrity of the PEGylated peptide across all spin-freezing conditions and excipient systems (Fig. 5A). Under refrigerated storage (2–8 °C), peptide levels remained stable with nearly 100 % over time, indicating that low-temperature storage effectively prevents degradation and maintains peptide integrity.

Fig. 2. Cake appearance of samples stored at 2–8 °C for 13 weeks. From left to right: Trehalose, Mannitol, and Sucrose–Mannitol formulations. Each set of four vials represents one formulation processed under different spin-freezing conditions: 5 °C/min, 592 W/kg; 50 °C/min, 592 W/kg; 5 °C/min, 5921 W/kg; 50 °C/min, 5921 W/kg.

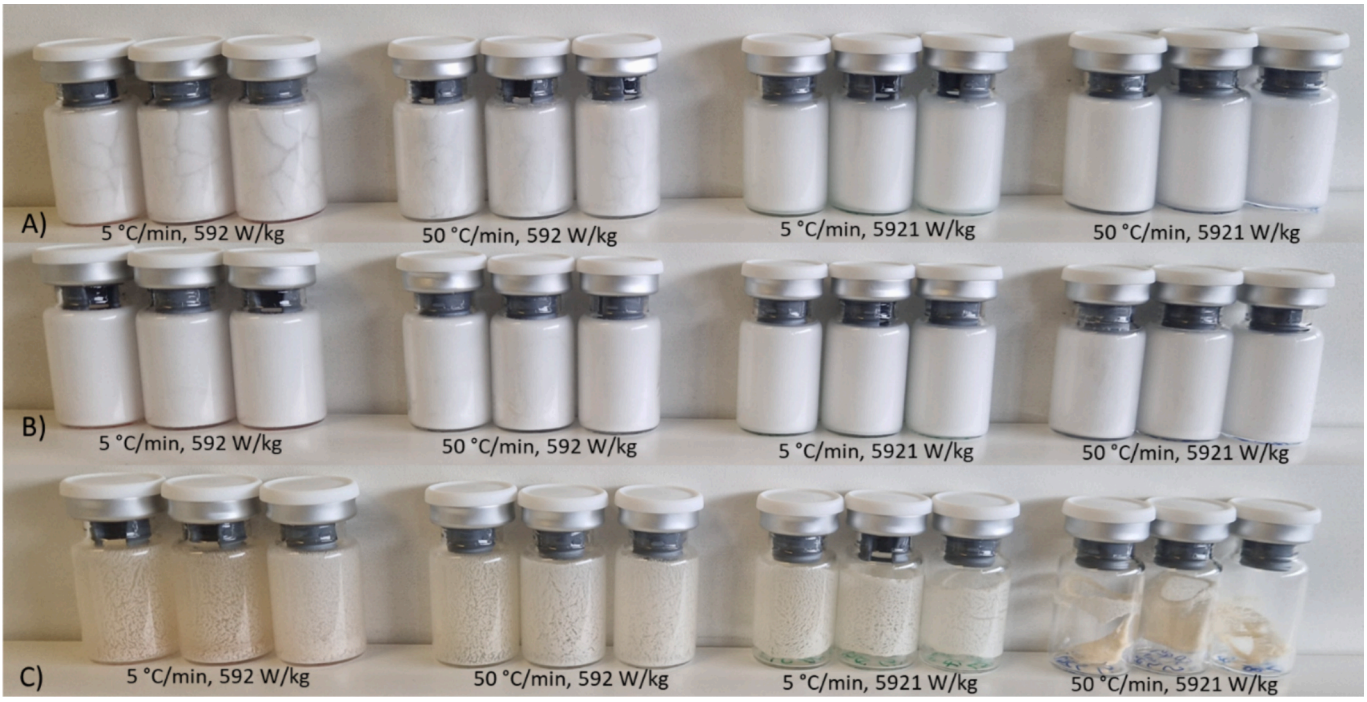

Fig. 3. Cake appearance in function of spin-freezing conditions in A) trehalose, B) mannitol, and C) sucrose-mannitol samples (triplicate) after 13 weeks at 50 °C.

Fig. 4. Cake appearance of A) freshly spin-frozen samples and B) samples stored at −70 °C prior to drying. Each set shows, from left to right, trehalose, mannitol, and sucrose–mannitol formulations processed under 5 °C/min, 592 W/kg and 50 °C/min, 5921 W/kg.

Two-way ANOVAs conducted at t_0 to assess the effects of cooling and ice crystallization conditions revealed no significant differences at t_0. For the trehalose formulation, neither cooling ($p = 0.827$) nor the controlled crystallization step during spin-freezing ($p = 0.255$) significantly affected peptide levels, and their interaction was also non-significant ($p = 0.623$). Similarly, for the mannitol formulation, the effects of the applied cooling ($p = 0.612$) and crystallization conditions ($p = 0.496$), and their interaction ($p = 0.570$) were not significant. In the sucrose–mannitol formulation, cooling ($p = 0.279$) and crystallization ($p = 0.179$) had no significant impact, and the interaction between these factors was non-significant as well ($p = 0.813$).

Due to the limited sample size at t_2 ($n = 1$ per condition), no reliable statistical evaluation could be performed at this timepoint. While apparent differences in peptide levels were observed in the trehalose

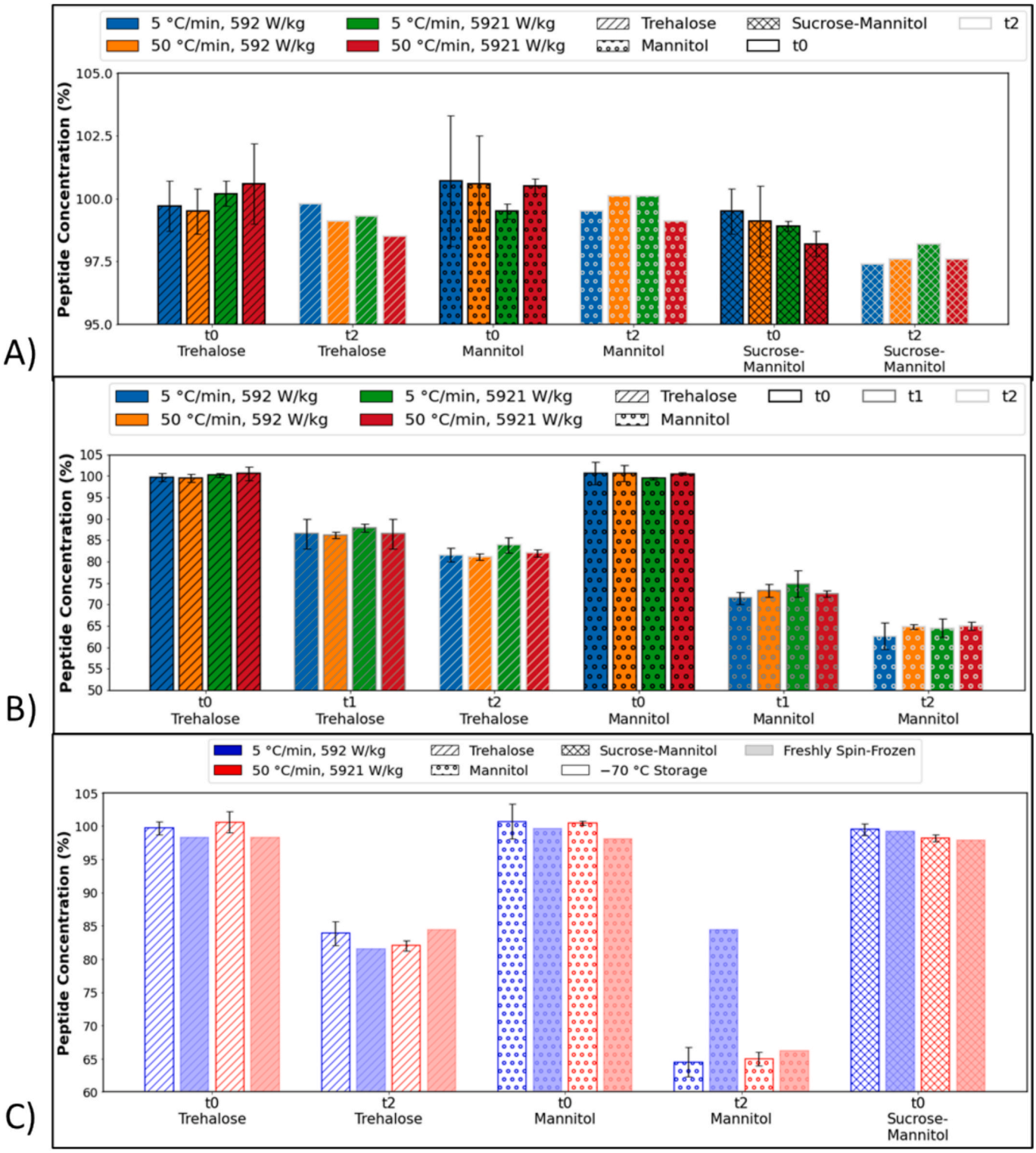

Fig. 5. Peptide concentration (%) across formulations and storage conditions. A) Peptide content at t_0 (immediately after drying) and t_2 (after 13 weeks at 2–8 °C) for trehalose, mannitol, and sucrose–mannitol samples processed under four spin-freezing conditions: 5 °C/min at 592 W/kg (blue), 50 °C/min at 592 W/kg (orange), 5 °C/min at 5921 W/kg (green), and 50 °C/min at 5921 W/kg (red). B) Peptide content at t_0, t_1 (after 6.5 weeks at 50 °C), and t_2 (after 13 weeks at 50 °C) for trehalose and mannitol samples under the same spin-freezing conditions. Sucrose–mannitol samples stored at 50 °C are excluded due to assay interference from Maillard-type degradation products. C) Peptide content at t_0 and t_2 (after 13 weeks at 50 °C) for samples processed under two spin-freezing conditions (5 °C/min, 592 W/kg and 50 °C/min, 5921 W/kg), comparing freshly spin-frozen vs. −70 °C pre-stored samples. Data are presented as mean ± SD (n = 3) at t_0; single-point measurements at t_1 and t_2 are shown without error bars.

formulation across cooling and crystallization conditions, these variations could not be robustly assessed due to the lack of replication. As such, no two-way ANOVAs were conducted at t_2, and any observed trends should be interpreted with caution, as they may reflect random variation rather than true effects. For both the mannitol and sucrose–mannitol formulations, similar observations at t_2 did not suggest consistent or meaningful patterns across conditions.

Following storage at 50 °C, distinct differences in peptide stability were observed between the formulations. In trehalose- and mannitol-based samples, peptide levels gradually declined over time (Fig. 5B). Mannitol formulations showed the most pronounced degradation, with concentrations dropping to ~63–75 % by the end of the study (t_2), while trehalose-based samples retained ~81–88 % of their initial content. This greater loss likely stems from mannitol crystallization during freezing, which phase–separates the peptide from the protective amorphous cake and weakens stabilizing API–excipient interactions (Cao et al., 2013).

To further evaluate the influence of spin-freezing parameters on peptide concentration, separate two-way ANOVAs were conducted at each time point (t_0, t_1, and t_2) for the trehalose and mannitol formulations. At t_0, neither the effect of cooling ($p = 0.806$) nor crystallization ($p = 0.213$) was significant, and their interaction was similarly non-significant ($p = 0.524$), indicating that variations did not influence the immediate post-drying peptide levels in these freezing parameters. At t_1, the analysis continued to show no significant effects, with p-values of 0.974 for cooling and 0.224 for crystallization, and the interaction remained non-significant ($p = 0.893$). At t_2, while the p-values for cooling ($p = 0.135$) and crystallization ($p = 0.092$) approached the significance threshold, neither parameters, nor their interaction ($p = 0.547$) reached statistical significance. Overall, the trehalose data suggest that, although there is a slight trend toward increased sensitivity at t_2, cooling and crystallization rates do not significantly alter peptide concentration.

In the mannitol formulation, the two-way ANOVA at t_0 revealed that cooling ($p = 0.537$) and crystallization ($p = 0.492$), as well as their interaction ($p = 0.570$), had no significant impact on peptide levels. Similarly, at t_1, the p-values for cooling ($p = 0.682$) and crystallization ($p = 0.465$) remained non-significant, and the interaction was also not significant ($p = 0.128$). At t_2, neither cooling ($p = 0.622$) nor crystallization ($p = 0.826$) showed significant effects, with the interaction also being non-significant ($p = 0.719$). Thus, for mannitol, the freezing parameters do not appear to influence peptide concentration at any of the timepoints evaluated. These results indicate that variations in cooling and crystallization rates do not influence peptide levels in either formulation; instead, formulation- and time-dependent degradation are the predominant factor under stress conditions.

In contrast, peptide quantification in the sucrose–mannitol formulation was markedly affected by storage-induced degradation processes that interfered with UV detection. Although apparent peptide concentrations remained high or even increased at later time points, these results were misleading. Chromatographic analysis revealed the presence of a large early-eluting peak at approximately 1.5 min and exaggerated main peak intensities at 280 nm, indicating the formation of UV-active degradation products with strong absorbance, thereby inflating the 280 nm signal.

These findings are consistent with known degradation pathways involving sucrose hydrolysis and Maillard-type reactions, with literature noting that sucrose at pH ≤ 5 poses a hydrolysis risk (Singh, 2018). Under acidic conditions and elevated temperatures, sucrose can hydrolyze into glucose and fructose. These reducing sugars are susceptible to further breakdown into aromatic compounds such as 5-hydroxymethylfurfural (HMF) and furans. As reported in previous works, HMF exhibits maximum absorbance at approximately 285 nm and typically elutes early in reversed-phase HPLC systems operating under mobile phase conditions with a high aqueous content (Ariffin et al., 2014; Martins et al., 2022). The peak detected at ~1.5 min aligns well with this behaviour and was only present in sucrose–mannitol samples stored at 50 °C, but not in refrigerated samples.

Simultaneously, reducing sugars formed via hydrolysis may engage in Maillard-type reactions with primary amine groups on the peptide, resulting in glycation products and advanced glycation end products (AGEs). These modifications introduce chromophores into the peptide structure, which contribute to the inflation of 280 nm absorbance. As shown in Fig. 6, only samples exposed to 50 °C exhibit strong absorbance around 280 nm, while samples stored at 2–8 °C remain unaffected. Literature provides strong evidence for this behaviour: Akhter et al. (Akhter et al., 2020) and Tang et al. (Tang et al., 2020) demonstrated that glycation of proteins (e.g., BSA, myoglobin), particularly with reactive carbonyl compounds such as methylglyoxal, results in progressive increases in 280 nm absorbance due to the formation of AGE-associated aromatic structures.

These findings directly support the UV changes observed here and indicate that the increased 280 nm signal is not reflective of intact peptide concentration but rather a result of Maillard-type reactions and AGE accumulation. The correlation between UV peak shifts, degraded chromatographic profiles, and physical changes such as cake browning further confirm glycation and sugar degradation as the root cause. Due to the pronounced interference from sugar-derived degradation products and glycated peptide species, absolute peptide quantification in sucrose–mannitol samples stored at 50 °C could not be reliably performed with the current RP-HPLC method, thus leading to the exclusion of the respective sucrose-mannitol results regarding peptide assay.

Across all formulations, spin-freezing conditions did not significantly impact peptide stability at any time point, indicating that variations in cooling and crystallization rates were not major contributors to degradation. Moreover, samples stored at −70 °C for several days prior to drying exhibited comparable peptide concentrations to freshly spin-frozen counterparts (Fig. 5C), confirming that short-term frozen storage does not affectphysical integrity under the applied conditions. However, since the freshly spin-frozen condition was assessed using only two vials per formulation, the data are insufficient for formal statistical analysis. While some variation was observed, such as a slightly lower recovery in the trehalose formulation at t_0, all values remained within the product-specific acceptable 95–105 % range. Given the limited sample size, these observations should be interpreted qualitatively and considered preliminary, guiding future investigations rather than supporting definitive conclusions.

In summary, while all formulations initially preserved peptide content post-lyophilization, their stability profiles diverged substantially under thermal stress. For systems containing reducing sugars, such as the sucrose–mannitol formulation, adaptations would be necessary. Alternative techniques, like liquid chromatography–mass spectrometry (LC-MS) may be suitable to accurately quantify peptide content in the presence of glycation and browning-related degradation products. Future studies should focus on optimizing drying protocols to reduce residual moisture and elevate the T_g, while also ensuring that storage conditions are carefully controlled in relation to the T_g to maximize formulation stability.

3.3. Monomer content

Size exclusion chromatography was used to evaluate the aggregation behaviour and monomer content of the PEGylated peptide across formulations and storage conditions. At the initial timepoint (t_0), all formulations displayed ~100 % monomer content, indicating successful lyophilization without aggregation or degradation/fragmentation (Fig. 7A).

Upon storage at 50 °C, distinct differences emerged between the formulations. The trehalose-based system retained the highest monomer fraction across all timepoints (>95 %), highlighting its ability to provide robust protection against aggregation. Mannitol-based samples showed substantial monomer loss (~10 – 12 %), suggesting increased susceptibility to thermal degradation while still retaining the majority of peptide

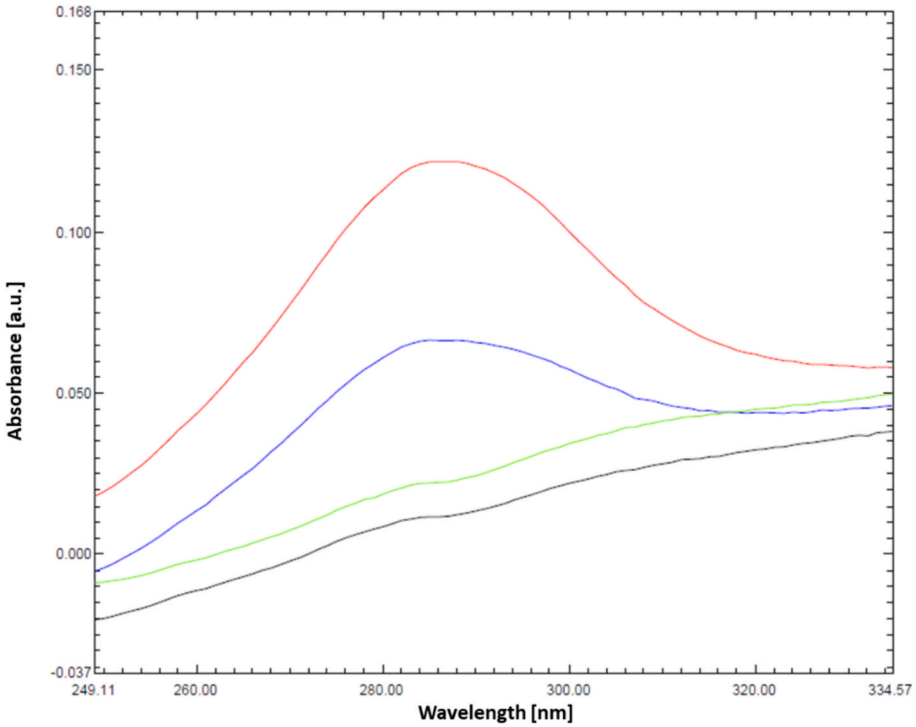

Fig. 6. UV spectra of reconstituted, 20-fold diluted sucrose–mannitol samples: initial sample right after drying (black), after 13 weeks at 2–8 °C (green), after 6.5 weeks at 50 °C (blue), and after 13 weeks at 50 °C (red).

in monomeric form. In contrast, the sucrose–mannitol formulation experienced the most pronounced drop in monomer content upon thermal stress (~45 %). This behaviour aligns with previous findings from RP-HPLC analysis and visual cake inspection, which revealed extensive degradation, browning, and collapse in the sucrose–mannitol formulation.

Notably, an additional peak at approximately 22 min was observed exclusively in the 280 nm chromatograms of sucrose–mannitol samples stored at 50 °C. The selective appearance of this peak at 280 nm strongly indicates the presence of aromatic degradation products, most likely 5–hydroxymethylfurfural (HMF), a sugar-derived compound commonly formed during sucrose degradation via Maillard reactions or caramelization. These findings complement those from RP-HPLC and UV spectroscopy in Section 3.2, which also demonstrated increased absorbance at 280 nm and the presence of early-eluting degradation peaks unique to sucrose–mannitol samples stored at 50 °C. Previous studies have shown that the formation of HMF is promoted under acidic and high-temperature conditions, particularly in the presence of glucose and fructose, which are generated upon sucrose hydrolysis (Assary et al., 2011; Martins et al., 2022; Zhang et al., 2019).

Although the RP-HPLC assay at 280 nm was compromised for sucrose–mannitol samples due to interference from degradation products, SEC analysis remains viable because it separates components primarily based on size and is less affected by overlapping UV signals. This enables more reliable quantification of the monomer fraction even in the presence of degradation products. This enables accurate quantification of the monomer fraction even in the presence of UV-active degradation products.

Furthermore, two-way ANOVAs were performed to evaluate the effect of freezing parameters (cooling and crystallization) on monomer content. At t_0, none of the factors significantly influenced monomer levels for any formulation (trehalose: $p = 0.827$ for cooling, $p = 0.255$ for crystallization, $p = 0.623$ for their interaction; mannitol: $p = 0.537$, $p = 0.492$, and $p = 0.570$, respectively; sucrose–mannitol: $p = 0.132$ for cooling and $p = 0.179$ for crystallization, with an interaction p-value of 0.813). At t_2, although trehalose samples showed a slight trend with crystallization approaching significance ($p \approx 0.092$) while cooling remained non-significant ($p \approx 0.135$), the mannitol and sucrose–mannitol formulations continued to show no significant effects (all $p > 0.51$). These statistical results support the conclusion that, under stress conditions, time-dependent degradation is the predominant factor affecting monomer stability, rather than differences in the freezing parameters.

In contrast, storage at 2–8 °C prevented the formation of degradation products, as indicated in Fig. 7B. All formulations retained nearly 100 % monomer content under refrigerated conditions, with no signs of aggregation or HMF-related peaks observed. Notably, the mannitol formulation exhibited the largest drop in monomer content (~2.5 %), suggesting it is more prone to aggregation than the sucrose–mannitol formulation when sucrose browning is limited. Additionally, while all formulations were stored far below their respective glass transition temperatures at 2–8 °C, the sucrose–mannitol formulation exhibited particularly enhanced stability under these conditions. Under refrigerated conditions, no notable differences in monomer content were observed across the different spin-freezing parameters for any of the formulations. This good stability is likely due to the storage temperature being well below the glass transition temperature ($T_g \sim 31$ °C) of the sucrose–mannitol formulation, thus limiting molecular mobility and degradation. In contrast, storage at 50 °C places the formulation above its Tg, increasing molecular mobility and susceptibility to degradation. Monomer levels remained within the product-specific acceptable 95–105 % range (corresponding to a cumulative degradation product limit below 5 %), suggesting that variations in cooling and crystallization rates did not have a meaningful impact on peptide stability. As these observations are based on single measurements per condition, they are interpreted qualitatively.

Additionally, no notable differences were observed between freshly spin-frozen samples and those stored at −70 °C for several days prior to drying (Fig. 7C), suggesting that short-term frozen storage before batch-drying does not substantially affect monomer content. For the sucrose–mannitol formulation at t_0, a slight difference in monomer fraction was observed between storage types; however, the absolute values

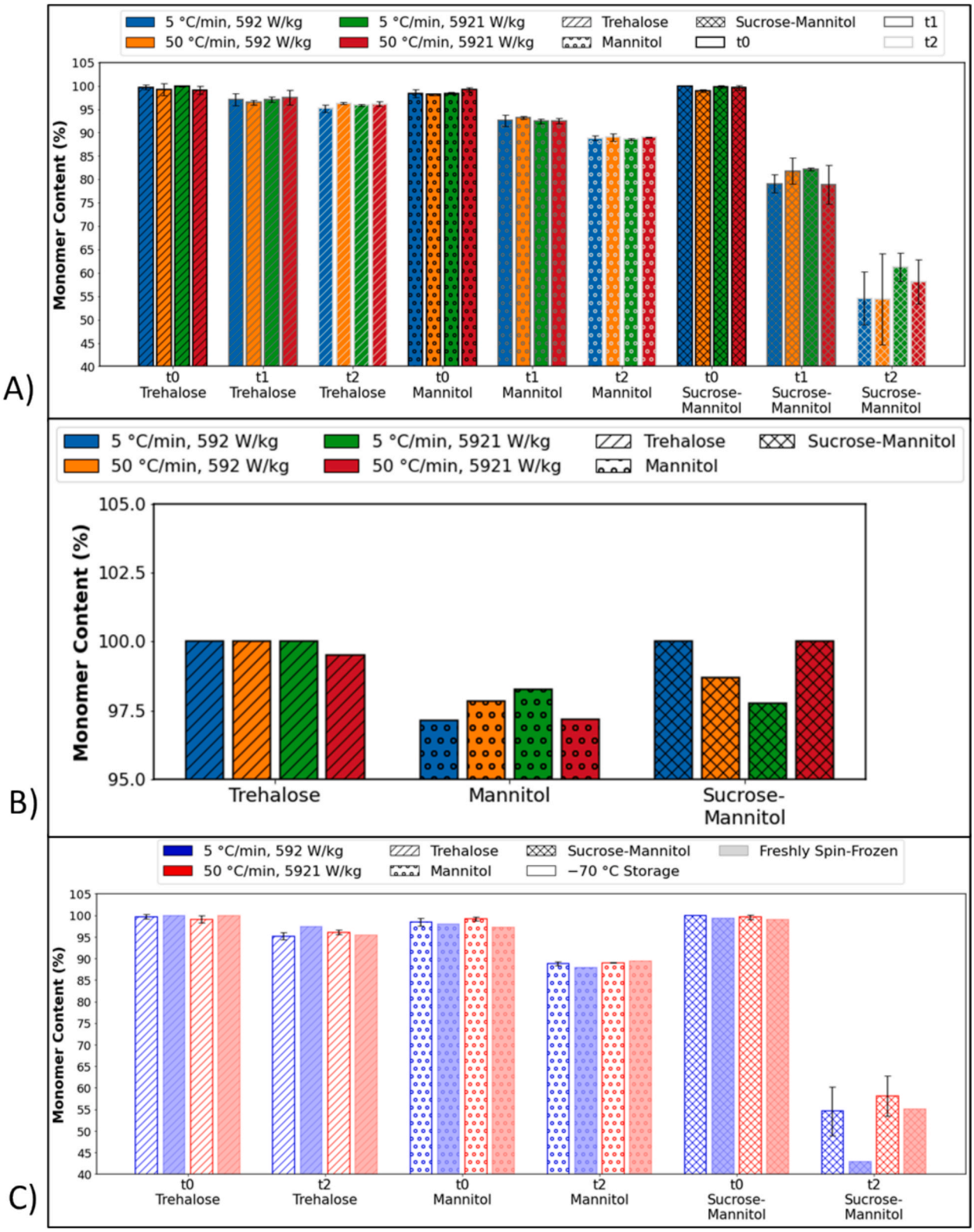

Fig. 7. Monomer content (%) across formulations, spin-freezing conditions, and storage settings. (A) Monomer content at t_0 (immediately after drying), t_1 (after 6.5 weeks at 50 °C), and t_2 (after 13 weeks at 50 °C) for trehalose, mannitol, and sucrose–mannitol formulations under four spin-freezing conditions: 5 °C/min at 592 W/kg (blue), 50 °C/min at 592 W/kg (orange), 5 °C/min at 5921 W/kg (green), and 50 °C/min at 5921 W/kg (red). Data are shown as mean ± SD. (B) Monomer content at t_2 (after 13 weeks at 2–8 °C) for the same formulations and processing conditions. Single measurements are shown (no error bars). (C) Monomer content at t_0 and t_2 (13 weeks at 50 °C) for samples processed under two spin-freezing conditions (5 °C/min, 592 W/kg and 50 °C/min, 5921 W/kg), comparing freshly spin-frozen vs. −70 °C pre-stored samples. t_0 values are triplicate means ± SD; t_2 values are single measurements.

remained within the product-specific acceptable 95–105 % range. No noticeable differences were observed for the mannitol and trehalose formulations at t_0, nor for any of the formulations at t_2. Given the limited replication for the freshly spin-frozen samples, these comparisons are interpreted qualitatively rather than as statistically conclusive.

The SEC results further support the interpretation that excipient selection and storage temperature are key drivers of peptide stability. While trehalose offered the most robust protection across all conditions, the sucrose–mannitol formulation was particularly susceptible to chemical degradation and aggregation under thermal stress. This instability was likely driven by the formation of reactive sugar-derived intermediates, (e.g., methylglyoxal), which can promote peptide aggregation through chemical modification and destabilization of the protein structure (Banerjee et al., 2016; Cardoso et al., 2023).

Notably, despite the distinct differences in cake appearance observed for the sucrose–mannitol samples in function of spin-freezing conditions (Section 3.1), these visual changes did not translate into significant variations in peptide concentration or monomer content; final assay results consistently remained within the product specific acceptable 95–105 % range. These findings suggest that, for this formulation, even if the sample morphology may appear compromised, the physical stability of the peptide is maintained under refrigerated storage conditions (2–8 °C).

4. Conclusion

This study demonstrates that formulation composition and storage temperature, rather than spin-freezing conditions, drive long-term stability in the freeze-dried PEGylated peptide formulations under investigation. Trehalose provided the most effective stabilization against thermal degradation, followed by mannitol, while the sucrose–mannitol formulation exhibited marked instability under stress conditions. The latter was characterized by cake collapse, browning, and peptide degradation, resulting from storage above the glass transition temperature and enhanced molecular mobility, which in turn was linked to high residual moisture content and a low glass transition temperature. While spin-freezing parameters and short-term frozen storage prior to drying had no measurable effect on product stability, the data underscore the importance of aligning formulation components with both product performance and analytical compatibility. These findings suggest that such systems not only require adapted analytical approaches but may also benefit from optimized drying protocols to reduce residual moisture and increase the T_g. In addition, maintaining storage temperatures in relation to the T_g is essential. Independent of our product-specific findings, continuous spin-freeze-drying has progressed from laboratory scale to a GMP-oriented prototype, and its continuous, modular, scale-out architecture supports prospective industrial application. Collectively, this work reinforces the need for an integrated approach to formulation, processing, and analysis to ensure the quality of freeze-dried biopharmaceutical therapeutics.

CRediT authorship contribution statement

Zarah Schaal: Writing – original draft, Visualization, Methodology, Investigation, Formal analysis, Conceptualization. **Pieter-Jan Van Bockstal:** Writing – review & editing, Methodology, Conceptualization. **Joris Lammens:** Methodology, Conceptualization. **Julian H. Lenger:** Writing – review & editing, Conceptualization. **Adrian P. Funke:** Writing – review & editing, Conceptualization. **Stefan C. Schneid:** Writing – review & editing, Conceptualization. **Thomas De Beer:** Methodology, Conceptualization.

Funding

This work was financed by Bayer AG.

Declaration of competing interest

The authors declare that they have no known competing financial interests or personal relationships that could have appeared to influence the work reported in this paper.

Data availability

Data will be made available on request.

References

Abla, K.K., Mehanna, M.M., 2022. Freeze-drying: a flourishing strategy to fabricate stable pharmaceutical and biological products. Int. J. Pharm. 628, 122233. https://doi.org/10.1016/J.IJPHARM.2022.122233.

Akhter, F., Chen, D., Akhter, A., Sosunov, A.A., Chen, A., McKhann, G.M., Yan, S.F., Yan, S.S.D., 2020. High dietary advanced glycation end products impair mitochondrial and cognitive function. J. Alzheimer's Dis. 76, 165–178. https://doi.org/10.3233/JAD-191236.

Al-Hussein, A., Gieseler, H., 2012. The effect of mannitol crystallization in mannitol–sucrose systems on LDH stability during freeze-drying. J. Pharm. Sci. 101, 2534–2544. https://doi.org/10.1002/JPS.23173.

Ariffin, A.A., Ghazali, H.M., Kavousi, P., 2014. Validation of a HPLC method for determination of hydroxymethylfurfural in crude palm oil. Food Chem. 154, 102–107. https://doi.org/10.1016/J.FOODCHEM.2013.12.082.

Assary, R.S., Redfern, P.C., Greeley, J., Curtiss, L.A., 2011. Mechanistic insights into the decomposition of fructose to hydroxy methyl furfural in neutral and acidic environments using high-level quantum chemical methods. J. Phys. Chem. B 115, 4341–4349. https://doi.org/10.1021/JP1104278.

Banerjee, S., Maity, S., Chakraborti, A.S., 2016. Methylglyoxal-induced modification causes aggregation of myoglobin. Spectrochim. Acta A Mol. Biomol. Spectrosc. 155, 1–10. https://doi.org/10.1016/J.SAA.2015.10.022.

Cao, W., Xie, Y., Krishnan, S., Lin, H., Ricci, M., 2013. Influence of process conditions on the crystallization and transition of metastable mannitol forms in protein formulations during lyophilization. Pharm. Res. 30, 131–139. https://doi.org/10.1007/S11095-012-0855-9/FIGURES/7.

Cardoso, H.B., Frommhagen, M., Wierenga, P.A., Gruppen, H., Schols, H.A., 2023. Maillard induced saccharide degradation and its effects on protein glycation and aggregation. Food Chem. Adv. 2, 100165. https://doi.org/10.1016/J.FOCHA.2022.100165.

Carpenter, J.F., Chang, B.S., Garzon-Rodriguez, W., Randolph, T.W., 2002. Rational design of stable lyophilized protein formulations: theory and practice. Pharm. Biotechnol. 13, 109–133. https://doi.org/10.1007/978-1-4615-0557-0_5.

De Meyer, L., Van Bockstal, P.J., Corver, J., Vervaet, C., Remon, J.P., De Beer, T., 2015. Evaluation of spin freezing versus conventional freezing as part of a continuous pharmaceutical freeze-drying concept for unit doses. Int. J. Pharm. 496, 75–85. https://doi.org/10.1016/j.ijpharm.2015.05.025.

Izutsu, K.I., 2018. Applications of freezing and freeze-drying in pharmaceutical formulations. Adv. Exp. Med. Biol. 1081, 371–383. https://doi.org/10.1007/978-981-13-1244-1_20.

Kasper, J.C., Friess, W., 2011. The freezing step in lyophilization: physico-chemical fundamentals, freezing methods and consequences on process performance and quality attributes of biopharmaceuticals. Eur. J. Pharm. Biopharm. https://doi.org/10.1016/j.ejpb.2011.03.010.

Kim, A.I., Akers, M.J., Nail, S.L., 1998. The physical state of mannitol after freeze-drying: effects of mannitol concentration, freezing rate, and a noncrystallizing cosolute. J. Pharm. Sci. 87, 931–935. https://doi.org/10.1021/JS980001D.

Lammens, J., Mortier, S.T.F.C., De Meyer, L., Vanbillemont, B., Van Bockstal, P.J., Van Herck, S., Corver, J., Nopens, I., Vanhoorne, V., De Geest, B.G., De Beer, T., Vervaet, C., 2018. The relevance of shear, sedimentation and diffusion during spin freezing, as potential first step of a continuous freeze-drying process for unit doses. Int. J. Pharm. 539, 1–10. https://doi.org/10.1016/J.IJPHARM.2018.01.009.

Leys, L., Vanbillemont, B., Van Bockstal, P.J., Lammens, J., Nuytten, G., Corver, J., Vervaet, C., De Beer, T., 2020. A primary drying model-based comparison of conventional batch freeze-drying to continuous spin-freeze-drying for unit doses. Eur. J. Pharm. Biopharm. 157, 97–107. https://doi.org/10.1016/J.EJPB.2020.09.009.

Martins, F.C.O.L., Alcantara, G.M.R.N., Silva, A.F.S., Melchert, W.R., Rocha, F.R.P., 2022. The role of 5-hydroxymethylfurfural in food and recent advances in analytical methods. Food Chem. 395, 133539. https://doi.org/10.1016/J.FOODCHEM.2022.133539.

Meyer, J.D., Nayar, R., Manning, M.C., 2009. Impact of bulking agents on the stability of a lyophilized monoclonal antibody. Eur. J. Pharm. Sci. 38, 29–38. https://doi.org/10.1016/J.EJPS.2009.05.008.

Nuytten, G., Revatta, S.R., Van Bockstal, P.J., Kumar, A., Lammens, J., Leys, L., Vanbillemont, B., Corver, J., Vervaet, C., De Beer, T., 2021. Development and application of a mechanistic cooling and freezing model of the spin freezing step within the framework of continuous freeze-drying. Pharmaceutics 13. https://doi.org/10.3390/pharmaceutics13122076.

Schaal, Z., Van Bockstal, P.J., Lammens, J., Lenger, J.H., Funke, A.P., Schneid, S.C., Svilenov, H.L., De Beer, T., 2025. Optimization of continuous spin-freeze-drying: the

role of spin-freezing on quality attributes and drying efficiency of a model peptide formulation. Eur. J. Pharm. Sci. 204. https://doi.org/10.1016/j.ejps.2024.106963.
Sharma, A., Khamar, D., Cullen, S., Hayden, A., Hughes, H., 2021. Innovative drying technologies for biopharmaceuticals. Int. J. Pharm. 609, 121115. https://doi.org/10.1016/J.IJPHARM.2021.121115.
Singh, S.K., 2018. Sucrose and trehalose in therapeutic protein formulations. AAPS Adv. Pharm. Sci. Series 38, 63–95. https://doi.org/10.1007/978-3-319-90603-4_3.
Tang, R., Faisal, M., Alatar, A.A., Alsaleh, A.N., Saeed, M., Ahmad, S., 2020. Glycation of heme-protein, "myoglobin" by 3-deoxyglucosone: Implications in immunogenicity. J. King Saud. Univ. Sci. 32, 2598–2602. https://doi.org/10.1016/j.jksus.2020.04.019.
Thakral, S., Sonje, J., Munjal, B., Bhatnagar, B., Suryanarayanan, R., 2023. Mannitol as an excipient for lyophilized injectable formulations. J. Pharm. Sci. 112, 19–35. https://doi.org/10.1016/J.XPHS.2022.08.029.
Zhang, L.L., Kong, Y., Yang, X., Zhang, Y.Y., Sun, B.G., Chen, H.T., Sun, Y., 2019. Kinetics of 5-hydroxymethylfurfural formation in the sugar-amino acid model of Maillard reaction. J. Sci. Food Agric. 99, 2340–2347. https://doi.org/10.1002/JSFA.9432.